
Large-Scale Optimization Algorithms for Sparse Conditional Gaussian Graphical Models

Calvin McCarter
Machine Learning Department
Carnegie Mellon University
calvinm@cmu.edu

Seyoung Kim
Lane Center for Computational Biology
Carnegie Mellon University
sssykim@cs.cmu.edu

Abstract

This paper addresses the problem of scalable optimization for l_1 -regularized conditional Gaussian graphical models. Conditional Gaussian graphical models generalize the well-known Gaussian graphical models to conditional distributions to model the output network influenced by conditioning input variables. While highly scalable optimization methods exist for sparse Gaussian graphical model estimation, state-of-the-art methods for conditional Gaussian graphical models are not efficient enough and more importantly, fail due to memory constraints for very large problems. In this paper, we propose a new optimization procedure based on a Newton method that efficiently iterates over two sub-problems, leading to drastic improvement in computation time compared to the previous methods. We then extend our method to scale to large problems under memory constraints, using block coordinate descent to limit memory usage while achieving fast convergence. Using synthetic and genomic data, we show that our methods can solve one million dimensional problems to high accuracy in a little over a day on a single machine.

1 Introduction

Sparse Gaussian graphical models (GGMs) [2] have been extremely popular as a tool for learning a network structure over a large number of continuous variables in many different application domains including neuroscience [7] and biology [2]. A sparse GGM can be estimated as a sparse inverse covariance matrix by minimizing the convex function of l_1 -regularized negative log-likelihood. Highly scalable learning algorithms such as glasso [2], QUIC [3], and BigQUIC [4] have been proposed to learn the model. Recently, sparse conditional Gaussian graphical models (CGGMs) [8, 10] have been receiving attention that extend GGMs to model a sparse network over outputs conditional on input variables, thus modeling structured outputs influenced by inputs. CGGMs can be viewed as a Gaussian analogue of conditional random field [6], while GGMs are a Gaussian analogue of Markov random field. A sparse CGGM can also be estimated by minimizing a convex function of l_1 -regularized negative log-likelihood. In this paper, we address the problem of scaling up the sparse CGGM estimation to a very large problem size.

Several different approaches have been proposed to estimate sparse CGGMs, including OWL-QN [8], accelerated proximal gradient [11], and Newton coordinate descent algorithm [10]. In particular, the Newton coordinate descent algorithm extends the QUIC algorithm for sparse GGM estimation to the case of CGGMs, and has been shown to have superior computational speed and convergence. This approach in each iteration finds a descent direction by minimizing a quadratic approximation of the original negative log-likelihood function along with l_1 regularization. Then, the parameter estimate is updated with this descent direction and a step size found by line search.

Although the Newton coordinate descent method is state-of-the-art for its fast convergence, it is still not efficient enough to be applied to many real-world problems with more than tens of thou-

sands of variables. More importantly, it suffers from a large space requirement, because for very high-dimensional problems, several large dense matrices need to be precomputed and stored during optimization. For a CGGM with p inputs and q outputs, the algorithm requires storing several $p \times p$ and $q \times q$ dense matrices, which cannot fit in memory for large p and q .

In this paper, we propose an optimization method for l_1 -regularized CGGMs, called an alternating Newton coordinate descent algorithm, that significantly speeds up the previous Newton coordinate descent algorithm. Our approach is based on the observation that it is not necessary to form a second-order approximation on all parameters as in the Newton coordinate descent algorithm, because given the parameters for output network structure, we can easily optimize over the other set of the parameters for mapping inputs to outputs. Thus, instead of performing a descent on all parameters simultaneously, we alternately optimize over each of the two sets of parameters. We show that our approach simplifies many aspects of the computation, significantly reducing computation time.

We further extend our approach to alternating Newton block coordinate descent to handle the space requirement, so that it can be applied to problems of any sizes on a machine with limited memory. Block-wise parameter updates were previously used in BigQUIC [4] for learning a sparse GGM, where the block sparsity pattern of the network parameters was leveraged to overcome the space limitations. We adopt their key idea and propose a strategy for dividing the parameters into blocks for block-wise updates such that the computation can be grouped and reused within each block.

2 Background

In this section, we provide a brief review of sparse CGGMs and learning algorithms for the model.

The Conditional Gaussian Graphical Model A CGGM [8, 10] models the conditional probability density of $\mathbf{x} \in \mathbb{R}^p$ given $\mathbf{y} \in \mathbb{R}^q$ as follows:

$$p(\mathbf{y}|\mathbf{x}; \mathbf{\Lambda}, \mathbf{\Theta}) = \exp\{-\mathbf{y}^T \mathbf{\Lambda} \mathbf{y} - 2\mathbf{x}^T \mathbf{\Theta} \mathbf{y}\} / Z(\mathbf{x}),$$

where $\mathbf{\Lambda}$ is a $q \times q$ matrix for modeling the network over \mathbf{y} and $\mathbf{\Theta}$ is a $p \times q$ matrix for modeling the mapping between the input variables \mathbf{x} and output variables \mathbf{y} . The normalization constant is given as $Z(\mathbf{x}) = c|\mathbf{\Lambda}|^{-1} \exp(\mathbf{x}^T \mathbf{\Theta} \mathbf{\Lambda}^{-1} \mathbf{\Theta}^T \mathbf{x})$. A CGGM can be viewed as a model derived from GGM for conditional distributions that represents the network over outputs \mathbf{y} influenced by inputs \mathbf{x} .

Given a dataset of $\mathbf{X} \in \mathbb{R}^{n \times p}$ and $\mathbf{Y} \in \mathbb{R}^{n \times q}$ for n samples, and their covariance matrices $\mathbf{S}_{\mathbf{xx}} = \frac{1}{n} \mathbf{X}^T \mathbf{X}$, $\mathbf{S}_{\mathbf{xy}} = \frac{1}{n} \mathbf{X}^T \mathbf{Y}$, $\mathbf{S}_{\mathbf{yy}} = \frac{1}{n} \mathbf{Y}^T \mathbf{Y}$, a sparse estimate of CGGM parameters can be obtained by minimizing l_1 -regularized negative log-likelihood:

$$\min_{\mathbf{\Lambda} > 0, \mathbf{\Theta}} f(\mathbf{\Lambda}, \mathbf{\Theta}) = g(\mathbf{\Lambda}, \mathbf{\Theta}) + h(\mathbf{\Lambda}, \mathbf{\Theta}), \quad (1)$$

where $g(\mathbf{\Lambda}, \mathbf{\Theta}) = -\log |\mathbf{\Lambda}| + \text{tr}(\mathbf{S}_{\mathbf{yy}} \mathbf{\Lambda} + 2\mathbf{S}_{\mathbf{xy}}^T \mathbf{\Theta} + \mathbf{\Lambda}^{-1} \mathbf{\Theta}^T \mathbf{S}_{\mathbf{xx}} \mathbf{\Theta})$ for the smooth negative log-likelihood and $h(\mathbf{\Lambda}, \mathbf{\Theta}) = \lambda_{\mathbf{\Lambda}} \|\mathbf{\Lambda}\|_1 + \lambda_{\mathbf{\Theta}} \|\mathbf{\Theta}\|_1$ for the non-smooth elementwise l_1 penalty. $\lambda_{\mathbf{\Lambda}}, \lambda_{\mathbf{\Theta}} > 0$ are regularization parameters. As observed in previous work, this objective is convex.

Optimization The current state-of-the-art method for solving Eq. (1) for l_1 -regularized CGGM is the Newton coordinate descent algorithm [10] that extends QUIC [3] for l_1 -regularized GGM estimation. In each iteration, this algorithm found a generalized Newton descent direction by forming a second-order approximation of the smooth part of the objective and minimizing this along with the l_1 penalty using a coordinate descent method. Given this Newton direction, the parameter estimates were updated with a step size found by line search using Armijo's rule [1].

In each iteration, the Newton coordinate descent algorithm found the Newton direction as follows:

$$\mathbf{D}_{\mathbf{\Lambda}}, \mathbf{D}_{\mathbf{\Theta}} = \underset{\Delta_{\mathbf{\Lambda}}, \Delta_{\mathbf{\Theta}}}{\text{argmin}} \bar{g}_{\mathbf{\Lambda}, \mathbf{\Theta}}(\Delta_{\mathbf{\Lambda}}, \Delta_{\mathbf{\Theta}}) + h(\mathbf{\Lambda} + \Delta_{\mathbf{\Lambda}}, \mathbf{\Theta} + \Delta_{\mathbf{\Theta}}), \quad (2)$$

where $\bar{g}_{\mathbf{\Lambda}, \mathbf{\Theta}}$ is the second-order approximation of g given by Taylor expansion:

$$\bar{g}_{\mathbf{\Lambda}, \mathbf{\Theta}}(\Delta_{\mathbf{\Lambda}}, \Delta_{\mathbf{\Theta}}) = \text{vec}(\nabla g(\mathbf{\Lambda}, \mathbf{\Theta}))^T \text{vec}([\Delta_{\mathbf{\Lambda}} \ \Delta_{\mathbf{\Theta}}]) + \frac{1}{2} \text{vec}([\Delta_{\mathbf{\Lambda}} \ \Delta_{\mathbf{\Theta}}])^T \nabla^2 g(\mathbf{\Lambda}, \mathbf{\Theta}) \text{vec}([\Delta_{\mathbf{\Lambda}} \ \Delta_{\mathbf{\Theta}}]).$$

The gradient and Hessian matrices above are given as:

$$\nabla g(\mathbf{\Lambda}, \mathbf{\Theta}) = \begin{bmatrix} \nabla_{\mathbf{\Lambda}} g(\mathbf{\Lambda}, \mathbf{\Theta}) & \nabla_{\mathbf{\Theta}} g(\mathbf{\Lambda}, \mathbf{\Theta}) \end{bmatrix} = [\mathbf{S}_{\mathbf{yy}} - \mathbf{\Sigma} - \mathbf{\Psi} \quad 2\mathbf{S}_{\mathbf{xy}} + 2\mathbf{\Gamma}] \quad (3)$$

$$\nabla^2 g(\mathbf{\Lambda}, \mathbf{\Theta}) = \begin{bmatrix} \nabla_{\mathbf{\Lambda}}^2 g(\mathbf{\Lambda}, \mathbf{\Theta}) & \nabla_{\mathbf{\Lambda}} \nabla_{\mathbf{\Theta}} g(\mathbf{\Lambda}, \mathbf{\Theta}) \\ \nabla_{\mathbf{\Lambda}} \nabla_{\mathbf{\Theta}} g(\mathbf{\Lambda}, \mathbf{\Theta})^T & \nabla_{\mathbf{\Theta}}^2 g(\mathbf{\Lambda}, \mathbf{\Theta}) \end{bmatrix} = \begin{bmatrix} \mathbf{\Sigma} \otimes (\mathbf{\Sigma} + 2\mathbf{\Psi}) & -2\mathbf{\Sigma} \otimes \mathbf{\Gamma}^T \\ -2\mathbf{\Sigma} \otimes \mathbf{\Gamma} & 2\mathbf{\Sigma} \otimes \mathbf{S}_{\mathbf{xx}} \end{bmatrix}, \quad (4)$$

where $\Sigma = \Lambda^{-1}$, $\Psi = \Sigma \Theta^T \mathbf{S}_{\text{xx}} \Theta \Sigma$, and $\Gamma = \mathbf{S}_{\text{xx}} \Theta \Sigma$. Given the Newton direction in Eq. (2), the parameters can be updated as $\Lambda \leftarrow \Lambda + \alpha \mathbf{D}_\Lambda$ and $\Theta \leftarrow \Theta + \alpha \mathbf{D}_\Theta$, where step size $0 < \alpha \leq 1$ ensures sufficient decrease in Eq. (1) and positive definiteness of Λ .

The *Lasso* problem [9] in Eq. (2) was solved using coordinate descent. Despite the efficiency of coordinate descent for *Lasso*, applying coordinate updates repeatedly to all $q^2 + pq$ variables in Λ and Θ is costly. So, the updates were restricted to an active set of variables given as:

$$\begin{aligned} \mathcal{S}_\Lambda &= \{(\Delta_\Lambda)_{ij} : |(\nabla_\Lambda g(\Lambda, \Theta))_{ij}| > \lambda_\Lambda \vee \Lambda_{ij} \neq 0\} \\ \mathcal{S}_\Theta &= \{(\Delta_\Theta)_{ij} : |(\nabla_\Theta g(\Lambda, \Theta))_{ij}| > \lambda_\Theta \vee \Theta_{ij} \neq 0\}. \end{aligned}$$

Because the active set sizes $m_\Lambda = |\mathcal{S}_\Lambda|$, $m_\Theta = |\mathcal{S}_\Theta|$ approach the number of non-zero entries in the sparse solutions for Λ^* and Θ^* over iterations, this strategy yields a substantial speedup.

To improve the efficiency of coordinate descent, Wytock and Kolter [10] proposed storing intermediate results for the large matrix products that need to be computed repeatedly. They computed and stored $\mathbf{U} := \Delta_\Lambda \Sigma$ and $\mathbf{V} := \Delta_\Theta \Sigma$ at the beginning of the optimization for Eq. (2). Then, after a coordinate descent update to $(\Delta_\Lambda)_{ij}$, row i and j of \mathbf{U} were updated. Similarly, after an update to $(\Delta_\Theta)_{ij}$, row i of \mathbf{V} was updated. We provide details of the coordinate descent update equations of this algorithm in Appendix.

Computational Complexity and Scalability At the beginning of the optimization in Eq. (2), large dense matrices Σ , Ψ , and Γ , for computing the gradient and Hessian in Eqs. (3) and (4), are precomputed and reused throughout the coordinate descent iterations. Initializing $\Sigma = \Lambda^{-1}$ via Cholesky decomposition costs up to $O(q^3)$ time. Computing $\Psi = \mathbf{R}^T \mathbf{R}$, where $\mathbf{R} = \mathbf{X} \Theta \Sigma$, requires $O(nm_\Theta + nq^2)$ time, and computing Γ costs $O(npq + nq^2)$. After the initializations, the cost of coordinate descent update per each active variable $(\Delta_\Lambda)_{ij}$ and $(\Delta_\Theta)_{ij}$ is $O(p + q)$. In practice, sparse Cholesky decomposition exploits sparsity to invert Λ in much less than $O(q^3)$, so the cost of pre-computing Ψ and Γ in $O(npq + nq^2)$ dominates.

A serious obstacle to scaling up to problems with large p and q is the space complexity for dense matrices Σ (size $q \times q$), Ψ (size $q \times q$), and Γ (size $p \times q$). In our experiments on a machine with 104 Gb RAM, the Newton coordinate descent method exhausted memory when $p + q$ exceeded 80,000.

In Section 3, we propose a modification of the Newton coordinate descent algorithm that significantly improves the computation time. Then, in Section 4, we show how block coordinate descent updates can remove the limitation on memory to scale it up to very large problems.

3 Alternating Newton Coordinate Descent

In this section, we introduce our alternating Newton coordinate descent algorithm for learning an l_1 -regularized CGGM that greatly reduces computation time compared to the previous method. Instead of performing Newton descent for all parameters Λ and Θ simultaneously, our approach alternately updates Λ and Θ , optimizing Eq. (1) over Λ given Θ and vice versa until convergence.

Our approach is based on the key observation that with Λ fixed, the problem of solving Eq. (1) over Θ becomes simply minimizing a quadratic function with l_1 regularization. Thus, it can be solved efficiently using a coordinate descent method, without the need to form a second-order approximation or to perform line search. Optimizing Eq. (1) for Λ given Θ still requires forming a quadratic approximation to find a generalized Newton direction and performing line search to find the step size. However, this computation is significantly simpler than performing the same type of computation on both Λ and Θ jointly as in the previous approach [10].

Coordinate Descent Optimization for Λ Given fixed Θ , the problem of minimizing the objective in Eq. (1) with respect to Λ becomes

$$\operatorname{argmin}_{\Lambda \succ 0} g_\Theta(\Lambda) + \lambda_\Lambda \|\Lambda\|_1, \quad (5)$$

where $g_\Theta(\Lambda) = -\log |\Lambda| + \operatorname{tr}(\mathbf{S}_{\text{yy}} \Lambda + \Lambda^{-1} \Theta^T \mathbf{S}_{\text{xx}} \Theta)$. In order to solve this, we first find a generalized Newton direction that minimizes the l_1 -regularized quadratic approximation of $g_\Theta(\Lambda)$:

$$\mathbf{D}_\Lambda = \operatorname{argmin}_{\Delta_\Lambda} \bar{g}_{\Lambda, \Theta}(\Delta_\Lambda) + \lambda_\Lambda \|\Lambda + \Delta_\Lambda\|_1, \quad (6)$$

Algorithm 1: Alternating Newton Coordinate Descent

input : Inputs $X \in \mathbb{R}^{n \times p}$ and $Y \in \mathbb{R}^{n \times q}$; regularization parameters $\lambda_\Lambda, \lambda_\Theta$

output: Parameters Λ, Θ

Initialize $\Theta \leftarrow 0, \Lambda \leftarrow I_q$

for $t = 0, 1, \dots$ **do**

 Determine active sets $\mathcal{S}_\Lambda, \mathcal{S}_\Theta$

 Solve via coordinate descent: $D_\Lambda = \arg \min_{\Delta_\Lambda, \Delta_{\bar{\mathcal{S}}_\Lambda=0}} \bar{g}_{\Lambda, \Theta}(\Lambda + \Delta_\Lambda, \Theta) + h(\Lambda + \Delta_\Lambda, \Theta)$

 Update $\Lambda^+ = \Lambda + \alpha D_\Lambda$, where step size α is found with line search

 Solve via coordinate descent: $\Theta^+ = \operatorname{argmin}_{\Theta_{\mathcal{S}_\Theta}} g_\Lambda(\Theta) + \lambda_\Theta \|\Theta\|_1$

where $\bar{g}_{\Lambda, \Theta}(\Delta_\Lambda)$ is obtained from a second-order Taylor expansion and is given as

$$\bar{g}_{\Lambda, \Theta}(\Delta_\Lambda) = \operatorname{vec}(\nabla_\Lambda g(\Lambda, \Theta))^T \operatorname{vec}(\Delta_\Lambda) + \frac{1}{2} \operatorname{vec}(\Delta_\Lambda)^T \nabla_\Lambda^2 g(\Lambda, \Theta) \operatorname{vec}(\Delta_\Lambda).$$

The $\nabla_\Lambda g(\Lambda, \Theta)$ and $\nabla_\Lambda^2 g(\Lambda, \Theta)$ above are components of the gradient and Hessian matrices corresponding to Λ in Eqs. (3) and (4). We solve the *Lasso* problem in Eq. (6) via coordinate descent. Similar to the Newton coordinate descent method, we maintain $\mathbf{U} := \Delta_\Lambda \Sigma$ to reuse intermediate results of the large matrix-matrix product. Given the Newton direction for Λ , we update $\Lambda \leftarrow \Lambda + \alpha \Delta_\Lambda$, where α is obtained by line search on the objective in Eq. (5).

Restricting the generalized Newton descent to Λ simplifies the computation significantly for coordinate descent updates, compared to the previous approach [10] that applies it to both Λ and Θ jointly. Our updates no longer involve $\nabla_\Theta g(\Lambda, \Theta)$ and $\nabla_\Lambda \nabla_\Theta g(\Lambda, \Theta)$, eliminating the need to compute the large $p \times q$ dense matrix Γ in $O(npq + nq^2)$ time. Our approach also reduces the computational cost for the coordinate descent update of each element of Δ_Λ from $O(p + q)$ to $O(q)$.

Coordinate Descent Optimization for Θ With Λ fixed, the optimization problem in Eq. (1) with respect to Θ becomes

$$\operatorname{argmin}_{\Theta} g_\Lambda(\Theta) + \lambda_\Theta \|\Theta\|_1, \quad (7)$$

where $g_\Lambda(\Theta) = \operatorname{tr}(2\mathbf{S}_{\mathbf{xy}}^T \Theta + \Lambda^{-1} \Theta^T \mathbf{S}_{\mathbf{xx}} \Theta)$. Since $g_\Lambda(\Theta)$ is a quadratic function itself, there is no need to form its second-order Taylor expansion or to determine a step size via line search. Instead, we solve Eq. (7) directly with coordinate descent method, storing and maintaining $\mathbf{V} := \Theta \Sigma$. Our approach reduces the computation time for updating Θ compared to the corresponding computation in the previous algorithm. We avoid computing the large $p \times q$ matrix Γ in each iteration, which had dominated overall computation time with $O(npq)$. Our approach also eliminates the need for line search for updating Θ . Finally, it reduces the cost for each coordinate descent update in Θ to $O(p)$, compared to $O(p + q)$ for the corresponding computation for Δ_Θ in the previous method.

Our approach is summarized in Algorithm 1. We provide the details of the coordinate descent update equations in Appendix. For approximately solving Eqs. (6) and (7), we warm-start Λ and Θ from the results of the previous iteration and make a single pass over the active set, which ensures decrease in the objective in Eq. (1) and reduces the overall computation time in practice.

4 Alternating Newton Block Coordinate Descent

The alternating Newton coordinate descent algorithm in the previous section improves the computation time of the previous state-of-the-art method, but is still limited by the space required to store large matrices during coordinate descent computation. Solving Eq. (6) for updating Λ requires pre-computing and storing $q \times q$ matrices, Σ and Ψ , whereas solving Eq. (7) for updating Θ requires Σ and a $p \times q$ matrix $\mathbf{S}_{\mathbf{xx}}$. A naive approach to reduce the memory footprint would be to recompute portions of these matrices on demand for each coordinate update, which would be very expensive.

In this section we describe how our algorithm in the previous section can be combined with block coordinate descent to scale up the optimization to very large problems on a machine with limited memory. During coordinate descent optimization, we update blocks of Δ_Λ and Δ_Θ so that within

Algorithm 2: Alternating Newton Block Coordinate Descent

input : Inputs $X \in \mathbb{R}^{n \times p}$ and outputs $Y \in \mathbb{R}^{n \times q}$; regularization parameters $\lambda_\Lambda, \lambda_\Theta$
output: Parameters Λ, Θ
Initialize $\Theta \leftarrow 0, \Lambda \leftarrow I_q$
for $t = 0, 1, \dots$ **do**
 Determine active sets $\mathcal{S}_\Lambda, \mathcal{S}_\Theta$
 Partition columns of Λ into k_Λ blocks ▷ Minimize over Λ
 Initialize $\Delta_\Lambda \leftarrow 0$
 for $z = 1$ to k_Λ **do**
 Compute $\Sigma_{C_z}, \mathbf{U}_{C_z}$, and Ψ_{C_z}
 for $r = 1$ to k_Λ **do**
 if $z \neq r$ **then**
 Identify columns $B_{zr} \subset C_r$ with active elements in Λ
 Compute $\Sigma_{B_{zr}}, \mathbf{U}_{B_{zr}}$, and $\Psi_{B_{zr}}$
 Update all active $(\Delta_\Lambda)_{ij}$ in (C_z, C_r)
 Update $\Lambda^+ \leftarrow \Lambda + \alpha \Delta_\Lambda$, where step size α is found by line search.
 Partition columns of Θ into k_Θ blocks ▷ Minimize over Θ
 for $r = 1$ to k_Θ **do**
 Compute Σ_{C_r} , and initialize $\mathbf{V} \leftarrow \Theta \Sigma_{C_r}$
 for row $i \in \{1, \dots, p\}$ if $I_\phi(\mathcal{S}_{(i, C_r)})$ **do**
 Compute $(\mathbf{S}_{\mathbf{xx}})_{ij}$ for non-empty rows j in V_{C_r}
 Update all active Θ_{ij} in (i, C_r)

each block, the computation of the large matrices can be cached and re-used, where these blocks are determined automatically by exploiting the sparse structure. For Δ_Λ , we extend the block coordinate descent approach in BigQUIC [4] developed for GGMs to take into account the conditioning variables in CGGMs. For Δ_Θ , we describe a new approach for block coordinate descent update. Our algorithm can, in principle, be applied to problems of any size on a machine with limited memory.

4.1 Blockwise optimization for Λ

Block coordinate descent method A coordinate-descent update of $(\Delta_\Lambda)_{ij}$ requires the i th and j th columns of Σ and Ψ . If these columns are in memory, they can be reused. Otherwise, it is a cache miss and we should compute them on demand. Σ_i for the i th column of Σ can be obtained by solving linear system $\Lambda \Sigma_i = \mathbf{e}_i$ with conjugate gradient method in $O(m_\Lambda K)$ time, where K is the number of conjugate gradient iterations. Then, Ψ_i can be obtained from $\mathbf{R}^T \mathbf{R}_i$, where $\mathbf{R} = \mathbf{X} \Theta \Sigma$.

In order to reduce cache misses, we perform block coordinate descent, where within each block, the columns of Σ are cached and re-used. Suppose we partition $\mathcal{N} = \{1, \dots, q\}$ into k_Λ blocks, $C_1, \dots, C_{k_\Lambda}$. We apply this partitioning to the rows and columns of Δ_Λ to obtain $k_\Lambda \times k_\Lambda$ blocks. We perform coordinate-descent updates in each block, updating all elements in the active set within that block. Let \mathbf{A}_{C_r} denote a q by $|C_r|$ matrix containing columns of Λ that corresponds to the subset C_r . In order to perform coordinate-descent updates on (C_r, C_z) block of Δ_Λ , we need Σ_{C_r} , Σ_{C_z} , Ψ_{C_r} , and Ψ_{C_z} . Thus, we pick the smallest possible k_Λ such that we can store $2q/k_\Lambda$ columns of Σ and $2q/k_\Lambda$ columns of Ψ in memory. When updating the variables within block (C_z, C_r) of Δ_Λ , there are no cache misses once Σ_{C_z} , Σ_{C_r} , Ψ_{C_z} , and Ψ_{C_r} are computed and stored. After updating each $(\Delta_\Lambda)_{ij}$ to $(\Delta_\Lambda)_{ij} + \mu$, we maintain \mathbf{U}_{C_z} and \mathbf{U}_{C_r} by $\mathbf{U}_{it} \leftarrow \mathbf{U}_{it} + \mu \Sigma_{jt}$, $\mathbf{U}_{jt} \leftarrow \mathbf{U}_{jt} + \mu \Sigma_{it}$, $\forall t \in \{C_z \cup C_r\}$.

To go through all blocks, we update blocks $(C_z, C_1), \dots, (C_z, C_k)$ for each $z \in \{1, \dots, k_\Lambda\}$. Since all of these blocks share Σ_{C_z} and Ψ_{C_z} , we precompute and store them in memory. When updating an off-diagonal block (C_z, C_r) , $z \neq r$, we compute Σ_{C_r} and Ψ_{C_r} . Overall, each block of Σ and Ψ will be computed k_Λ times.

Reducing computational cost using graph clustering In typical real-world problems, the graph structure of Λ will exhibit clustering, with an approximately block diagonal structure. We exploit

this structure by choosing a partition $\{C_1, \dots, C_{k_\Lambda}\}$ that reduces cache misses. Within diagonal blocks (C_r, C_r) 's, once Σ_{C_r} and Ψ_{C_r} are computed, there are no cache misses. For off-diagonal blocks (C_r, C_z) 's, $r \neq z$, we have a cache miss only if some variable in $\{\Delta_{ij} | i \in C_r, j \in C_z\}$ lies in the active set. We thus minimize the active set in off-diagonal blocks via clustering, following the strategy for sparse GGM estimation in [4]. We use the METIS [5] graph clustering library.

Although the worst-case scenario is to compute Σ and Ψ k_Λ times to update all elements of Δ_Λ , in practice, graph clustering dramatically reduces this additional cost of block-wise optimization. In the best case, if the active set for Λ is perfectly block-diagonal and graph clustering identifies this block diagonal structure, we need to compute Σ and Ψ only once to update all the blocks.

4.2 Blockwise Optimization for Θ

Block coordinate descent method The coordinate descent update of Θ_{ij} requires $(\mathbf{S}_{\mathbf{xx}})_i$ and Σ_j to compute $(\mathbf{S}_{\mathbf{xx}})_i^T \mathbf{V}_j$, where $\mathbf{V}_j = \Theta \Sigma_j$. If $(\mathbf{S}_{\mathbf{xx}})_i$ and Σ_j are not already in the memory, it is a cache miss. Computing $(\mathbf{S}_{\mathbf{xx}})_i$ takes $O(np)$, which is expensive if we have many cache misses.

We propose a block coordinate descent approach for solving Eq. (7) that groups these computations to reduce cache misses. Given a partition $\{1, \dots, q\}$ into k_Θ subsets, C_1, \dots, C_{k_Θ} , we divide Θ into $p \times k_\Theta$ blocks, where each block comprises a portion of a row of Θ . We denote each block (i, C_r) , where $i \in \{1, \dots, p\}$. Since updating block (i, C_r) requires $(\mathbf{S}_{\mathbf{xx}})_i$ and Σ_{C_r} , we pick smallest possible k_Θ such that we can store q/k_Θ columns of Σ in memory. While performing coordinate descent updates within block (i, C_r) of Θ , there are no cache misses, once $(\mathbf{S}_{\mathbf{xx}})_i$ and Σ_{C_r} are in memory. After updating each Θ_{ij} to $\Theta_{ij} + \mu$, we update \mathbf{V}_{C_r} by $\mathbf{V}_{it} \leftarrow \mathbf{V}_{it} + \mu \Sigma_{jt}, \forall t \in C_r$.

In order to sweep through all blocks, each time we select a $q \in \{1, \dots, k_\Theta\}$ and update blocks $(1, C_r), \dots, (p, C_r)$. Since all of these p blocks with the same C_r share the computation of Σ_{C_r} , we compute and store Σ_{C_r} in memory. Within each block, the computation of $(\mathbf{S}_{\mathbf{xx}})_i$ is shared, so we pre-compute and store it in memory, before updating this block. The full matrix of Σ will be computed once while sweeping through the full Θ , whereas $\mathbf{S}_{\mathbf{xx}}$ will be computed k_Θ times.

Reducing computational cost using row-wise sparsity We further reduce cache misses for $(\mathbf{S}_{\mathbf{xx}})_i$ by strategically selecting partition C_1, \dots, C_{k_Θ} , based on the observation that if the active set is empty in block (i, C_r) , we can skip this block and forgo computing $(\mathbf{S}_{\mathbf{xx}})_i$. We therefore choose a partition where the active set variables are clustered into as few blocks as possible. Formally, we want to minimize $\sum_{i,q} |I_\phi(\mathcal{S}_{(i,C_r)})|$, where $I_\phi(\mathcal{S}_{(i,C_r)})$ is an indicator function that outputs 1 if the active set $\mathcal{S}_{(i,C_r)}$ within block (i, C_r) is not empty and 0 otherwise. We therefore perform graph clustering over the graph $G = (V, E)$ defined from the active set in Θ , where $V = \{1, \dots, q\}$ with one node for each column of Θ , and $E = \{(j, k) | \Theta_{ij} \in \mathcal{S}_\Theta, \Theta_{ik} \in \mathcal{S}_\Theta \text{ for } i = 1, \dots, p\}$, connecting two nodes j and k with an edge if both Θ_{ij} and Θ_{ik} are in the active set. This edge set corresponds to the non-zero elements of $\Theta^T \Theta$, so the graph can be computed quickly in $O(m_\Theta q)$.

We also exploit row-wise sparsity in Θ to reduce the cost of each cache miss. Every empty row in Θ corresponds to an empty row in $\mathbf{V} = \Theta \Sigma$. Because we only need elements in $(\mathbf{S}_{\mathbf{xx}})_i$ for the dot product $(\mathbf{S}_{\mathbf{xx}})_i^T \mathbf{V}_j$, we skip computing the k th element of $(\mathbf{S}_{\mathbf{xx}})_i$ if the k th row of Θ is all zeros. Our method is summarized in Algorithm 2. See Appendix for analysis of the computational cost.

Parallelization Some of the expensive computations in our algorithm are embarrassingly-parallelizable on multi-core machines. We parallelize matrix multiplications and compute multiple columns of Σ_{C_r} in parallel. For Θ , we compute elements within each $\mathbf{S}_{\mathbf{xx}_i}$ in parallel.

5 Experiments

We compare the performance of our proposed methods with the existing state-of-the-art Newton coordinate descent algorithm, using synthetic and real-world genomic datasets. All methods were implemented in C++ with parameters represented in sparse matrix format. All experiments were run on 2.6GHz Intel Xeon E5 machines with 8 cores and 104 Gb RAM, running Linux OS. We run the Newton coordinate descent and alternating Newton coordinate descent algorithms as a single thread job on a single core. For our alternating Newton block coordinate descent method, we run it on a single core and with parallelization on 8 cores.

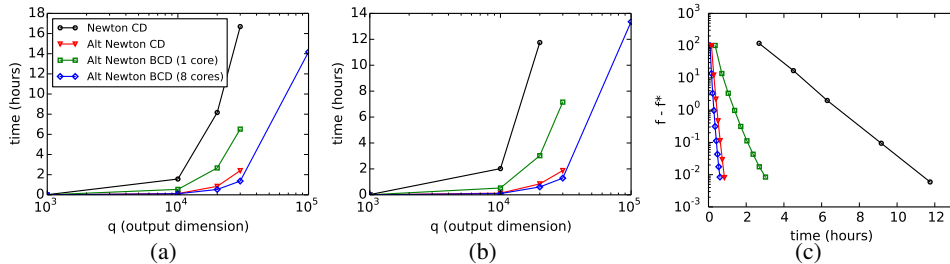


Figure 1: Comparison of scalability on chain graphs. We vary p and q , where (a) $p = q$ and (b) $p = 2q$. The Newton coordinate descent and alternating Newton coordinate descent methods could not be run beyond the problem sizes shown due to memory constraint. (c) Convergence when $q = 20,000$ and $p = 40,000$.

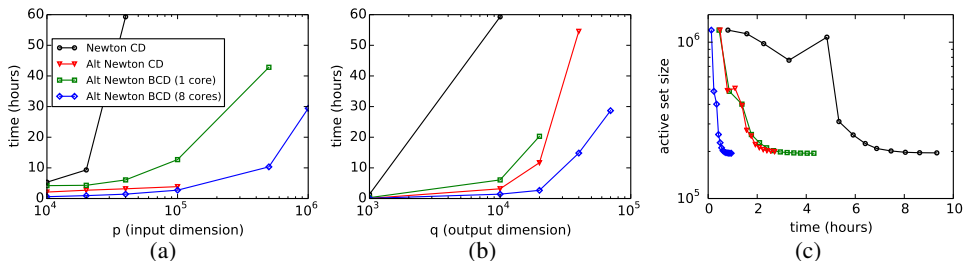


Figure 2: Comparison of scalability on random graphs with clustering. (a) Varying p with q fixed at 10,000. (b) Varying q with p fixed at 40,000. (c) Active set size versus time with $p = 20,000$ and $q = 10,000$.

5.1 Synthetic Experiments

We compare the different methods on two sets of synthetic datasets, one for chain graphs and another for random graphs with clustering for Λ , generated as follows. For chain graphs, the true sparse parameters Λ is set with $\Lambda_{i,i-1} = 1$ and $\Lambda_{i,i} = 2.25$ and the ground truth Θ is set with $\Theta_{i,i} = 1$. We perform one set of chain graph experiments where the number of inputs p equals the number of outputs q , and another set of experiments with an additional q irrelevant features unconnected to any outputs, so that p equals $2q$. For random graphs with clustering, following the procedure in [4] for generating a GGM, we set the true Λ to a graph with clusters of nodes of size 250 and with 90% of edges connecting randomly-selected nodes within clusters. We set the number of edges so that the average degree of each node is 10, with edge weights set to 1. We then set the diagonal values so that Λ is positive definite. To set the sparse patterns for Θ , we randomly select $100\sqrt{p}$ input variables as having edges to at least one output and distribute total $10q$ edges among those selected inputs to influence randomly selected outputs. We set the edge weights of Θ to 1.

Then, we draw samples from the CGGM defined by these true Λ and Θ . We generate datasets with $n = 100$ samples for the chain graphs and $n = 200$ samples for random graphs with clustering. We choose λ_Λ and λ_Θ so that the number of estimated edges in Λ and Θ is close to ground truth. Following the strategy used in GGM estimation [4], we use the minimum-norm subgradient of the objective as our stopping criterion: $\|\text{grad}^S(\Lambda_t, \Theta_t)\|_1 < 0.01(\|\Lambda\|_1 + \|\Theta\|_1)$.

We compare the scalability of the different methods for chain graph experiments, as we vary the problem sizes. We show the computation times for datasets with $p = q$ in Figure 1(a) and for datasets with $p = 2q$ with q additional irrelevant features in Figure 1(b). For large problems, computation times are not shown for Newton coordinate descent and alternating Newton coordinate descent methods because they could not complete the optimization with limited memory. Also, for large problems, alternating block coordinate descent was terminated after 60 hours of computation. In Figure 1(c), using the dataset with $p = 40,000$ and $q = 20,000$, we plot the suboptimality in the objective $f - f^*$, where f^* is obtained by running alternating Newton coordinate descent algorithm to numerical precision. Our results show that all of our new methods converge substantially faster than the Newton coordinate descent method, regardless of desired accuracy level. We provide more results on varying the sample size n in Appendix.

In Figure 2, we compare scalability of different methods for random graphs with clustering. In Figure 2(a), we vary p , while setting q to 10,000. In Figure 2(b), we vary q , fixing p to 40,000. Similar to the results from chain graph, for larger problems, Newton coordinate descent and alternating

Table 1: Computation time in seconds on genomic dataset. “*” indicates running out of memory.

| p | q | $\ \Lambda^*\ _0$ | $\ \Theta^*\ _0$ | Newton CD | Alternating Newton CD | Alternating Newton BCD |
|---------|--------|-------------------|------------------|-----------|-----------------------|------------------------|
| 34,249 | 3,268 | 34,914 | 28,848 | 79,116 | 1,836 | 876 |
| 34,249 | 10,256 | 86,090 | 103,767 | > 180,000 | 8,637 | 8,119 |
| 442,440 | 3,268 | 26,232 | 30,482 | * | * | 39,549 |

Newton coordinate descent methods ran out of memory and alternating block coordinate descent was terminated after 60 hours. For all problem sizes, our alternating Newton coordinate descent algorithm significantly reduces the computation time of the previous method, the Newton coordinate descent algorithm. This gap in the computation time increases for larger problems. In Figure 2(c), we compare the convergence in sparsity pattern for the different methods as measured by the active set size, for problem size $p = 20,000$ and $q = 10,000$. All our methods recover the optimal sparsity pattern much more rapidly than the previous approach.

Figures 1 and 2 show that our alternating Newton block coordinate descent can run on much larger problems than any other methods, while those methods without block coordinate descent run out of memory. For example, in Figure 2(a) alternating Newton block coordinate descent could handle problems with one million inputs, while without block-wise optimization it ran out of memory when $p > 100,000$. We also notice that on a single core, the alternating Newton block coordinate descent is slightly slower than the same method without block-wise optimization because of the need to recompute Σ and S_{xx} . However, it is still substantially faster than the previous method.

Finally, we evaluate the parallelization scheme for our alternating Newton block coordinate descent method on multi-core machines. Given a dataset generated from chain graph with $p = 40,000$ and $q = 20,000$, in Figure 3, we show the folds of speedup for different numbers of cores with respect to a single core. We obtained about 7 times speed up with 8 cores on a machine with 104Gb RAM, and about 12 times speedup with 16 cores on a machine with 28Gb RAM.

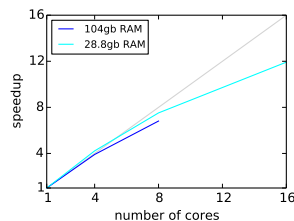


Figure 3: Speedup with parallelization for alternating Newton block coordinate descent.

5.2 Genomic Data Analysis

We compare the different methods on a genomic dataset. The dataset consists of genotypes for 442,440 single nucleotide polymorphisms (SNPs) and 10,256 gene expression levels for 171 individuals with asthma, after removing genes with variance under 0.01. We fit a sparse CGGM using SNPs as inputs and expressions as outputs to model a gene network influenced by SNPs. We also compared the methods on a smaller dataset of 34,249 SNPs from chromosome 1 and 3,268 genes with variance > 0.1 . As typically sparse model structures are of interests in this type of analysis, we chose regularization parameters so that the number of non-zero entries in each of Θ and Λ at convergence was approximately 10 times the number of genes.

The computation time of different methods are provided in Table 1. On the largest problem, the previous approach could not run due to memory constraint, whereas our block coordinate descent converged in around 11 hours. We also compare the convergence of the different methods on the dataset with 34,249 SNPs and 3,268 gene expressions in Figure 4, and find that our methods provide vastly superior convergence than the previous method.

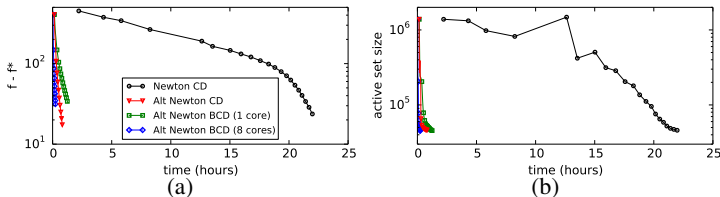


Figure 4: Convergence results on genomic dataset. (a) Suboptimality and (b) active set size over time on dataset with $p = 34,249$ and $q = 3,268$.

6 Conclusion

In this paper, we addressed the problem of large-scale optimization for sparse CGGMs. We proposed a new optimization procedure, called alternating Newton coordinate descent, that reduces computation time by alternately optimizing for the two sets of parameters Λ and Θ . Further, we extended this with block-wise optimization so that it can run on any machine with limited memory.

References

- [1] Larry Armijo et al. Minimization of functions having lipschitz continuous first partial derivatives. *Pacific Journal of mathematics*, 16(1):1–3, 1966.
- [2] J. Friedman, T. Hastie, and R. Tibshirani. Sparse inverse covariance estimation with the graphical lasso. *Biostatistics*, 9(3):432–441, 2008.
- [3] Cho-Jui Hsieh, Inderjit S. Dhillon, Pradeep K. Ravikumar, and Mátyás A. Sustik. Sparse inverse covariance matrix estimation using quadratic approximation. In *Advances in Neural Information Processing Systems 24*, pages 2330–2338. 2011.
- [4] Cho-Jui Hsieh, Matyas A Sustik, Inderjit S Dhillon, Pradeep K Ravikumar, and Russell Pol-drack. Big & quic: Sparse inverse covariance estimation for a million variables. In *Advances in Neural Information Processing Systems 26*, pages 3165–3173. 2013.
- [5] George Karypis and Vipin Kumar. Metis-unstructured graph partitioning and sparse matrix ordering system, version 2.0. 1995.
- [6] A. Lafferty, J. McCallum and F. Pereira. Conditional random fields: Probabilistic models for segmenting and labeling sequence data. In *Proceedings of the 18th International Conference on Machine Learning*, 2001.
- [7] Bernard Ng, Rafeef Abugharbieh, Gael Varoquaux, Jean Baptiste Poline, and Bertrand Thirion. Connectivity-informed fmri activation detection. In *Medical Image Computing and Computer-Assisted Intervention–MICCAI 2011*, pages 285–292. Springer, 2011.
- [8] K.A. Sohn and S. Kim. Joint estimation of structured sparsity and output structure in multiple-output regression via inverse-covariance regularization. In *Proceedings of the 15th International Conference on Artificial Intelligence and Statistics (AISTATS)*, volume 16. JMLR W&CP, 2012.
- [9] R. Tibshirani. Regression shrinkage and selection via the lasso. *Journal of Royal Statistical Society, Series B*, 58(1):267–288, 1996.
- [10] M. Wytock and J.Z. Kolter. Sparse gaussian conditional random fields: algorithms, theory, and application to energy forecasting. In *Proceedings of the 30th International Conference on Machine Learning*, volume 28. JMLR W&CP, 2013.
- [11] Xiao-Tong Yuan and Tong Zhang. Partial gaussian graphical model estimation. *IEEE Transactions on Information Theory*, 60(3):1673–1687, 2014.

A Appendix

A.1 Coordinate Descent Updates for Newton Coordinate Descent Method

In this section, we provide details of the coordinate-descent update equations for the Newton coordinate descent algorithm. In the Newton coordinate descent method, the coordinate-descent method for computing a generalized Newton direction iteratively updates each element of Δ_Λ as follows:

$$(\Delta_\Lambda)_{ij} \leftarrow (\Delta_\Lambda)_{ij} - c_\Lambda + S_{\lambda_\Lambda/a_\Lambda}(c_\Lambda - \frac{b_\Lambda}{a_\Lambda}),$$

where $S_r(w) = \text{sign}(w) \max(|w| - r, 0)$ is the soft-thresholding operator and

$$\begin{aligned} a_\Lambda &= \Sigma_{ij}^2 + \Sigma_{ii}\Sigma_{jj} + \Sigma_{ii}\Psi_{jj} + 2\Sigma_{ij}\Psi_{ii} \\ b_\Lambda &= (\mathbf{S}_{yy})_{ij} - \Sigma_{ij} - \Psi_{ij} + (\Sigma\Delta_\Lambda\Sigma)_{ij} - \Phi_{ij} - \Phi_{ji} + (\Psi\Delta_\Lambda\Sigma)_{ij} + (\Psi\Delta_\Lambda\Sigma)_{ji} \\ c_\Lambda &= \Lambda_{ij} + (\Delta_\Lambda)_{ij} \end{aligned}$$

given $\Sigma = \Lambda^{-1}$, $\Psi := \Sigma\Theta^T\mathbf{S}_{xx}\Theta\Sigma$, and $\Phi := \Sigma\Theta^T\mathbf{S}_{xx}\Delta_\Theta\Sigma$.

Similarly, in each coordinate-descent iteration, each element of Δ_Θ is updated as follows:

$$(\Delta_\Theta)_{ij} \leftarrow (\Delta_\Theta)_{ij} - c_\Theta + S_{\lambda_\Theta/a_\Theta}(c_\Theta - \frac{b_\Theta}{a_\Theta}),$$

where

$$\begin{aligned} a_\Theta &= \Sigma_{jj}(\mathbf{S}_{xx})_{ii} \\ b_\Theta &= 2(\mathbf{S}_{xy})_{ij} + 2(\mathbf{S}_{xx}\Theta\Sigma)_{ij} + 2(\mathbf{S}_{xx}\Delta_\Theta\Sigma)_{ij} - 2(\mathbf{S}_{xx}\Theta\Sigma\Delta_\Lambda\Sigma)_{ij} \\ c_\Theta &= \Theta_{ij} + (\Delta_\Theta)_{ij}. \end{aligned}$$

A.2 Coordinate Descent Updates for Alternating Newton Coordinate Descent Method

In our alternating Newton coordinate descent algorithm, during coordinate-descent optimization for computing a generalized Newton direction, each element of Δ_Λ is updated as follows:

$$(\Delta_\Lambda)_{ij} \leftarrow (\Delta_\Lambda)_{ij} - c_\Lambda + S_{\lambda_\Lambda/a_\Lambda}(c_\Lambda - \frac{b_\Lambda}{a_\Lambda}),$$

where

$$\begin{aligned} a_\Lambda &= \Sigma_{ij}^2 + \Sigma_{ii}\Sigma_{jj} + \Sigma_{ii}\Psi_{jj} + 2\Sigma_{ij}\Psi_{ii} \\ b_\Lambda &= (\mathbf{S}_{yy})_{ij} - \Sigma_{ij} - \Psi_{ij} + (\Sigma\Delta_\Lambda\Sigma)_{ij} + (\Psi\Delta_\Lambda\Sigma)_{ij} + (\Psi\Delta_\Lambda\Sigma)_{ji} \\ c_\Lambda &= \Lambda_{ij} + (\Delta_\Lambda)_{ij}. \end{aligned}$$

For Θ , we perform coordinate-descent updates directly on Θ without forming a second-order approximation of the log-likelihood to find a Newton direction, as follows:

$$\Theta_{ij} \leftarrow \Theta_{ij} - c_\Theta + S_{\lambda_\Theta/a_\Theta}(c_\Theta - \frac{b_\Theta}{a_\Theta}),$$

where

$$\begin{aligned} a_\Theta &= \Sigma_{jj}(\mathbf{S}_{xx})_{ii} \\ b_\Theta &= 2(\mathbf{S}_{xy})_{ij} + 2(\mathbf{S}_{xx}\Theta\Sigma)_{ij} \\ c_\Theta &= \Theta_{ij}. \end{aligned}$$

A.3 Time Complexity Analysis of Alternating Newton Block Coordinate Descent

In this section we describe the time complexity of the alternating Newton block coordinate descent method. The active set sizes for Λ and Θ are m_Λ and m_Θ , respectively. Also, $K \sim 10$ is the average number of conjugate gradient iterations.

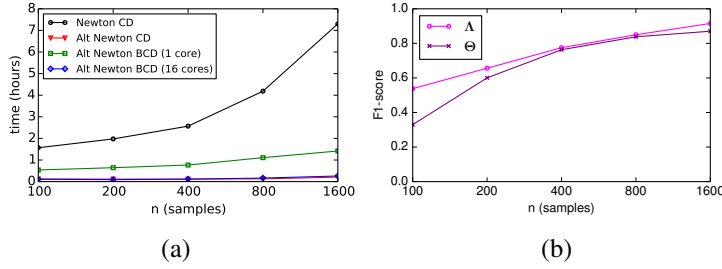


Figure 5: Results from synthetic data experiments. Data were generated from chain graph structure with $p = q = 10,000$. (a) Comparison of computation time of different methods for varying sample size n . (b) Comparison of edge recovery accuracy as measured by F_1 -score, for different sample sizes n .

A.3.1 Cost of updating Λ

The cost of computing Σ_{C_z} and Ψ_{C_z} for all $z \in \{1, \dots, k_\Lambda\}$ is $O(qm_\Lambda K)$ and $O(nq^2)$, respectively, regardless of sparsity in Λ . However, the cost of computing Σ_{C_r} and Ψ_{C_r} for all $z \neq r$ depends on the block-diagonal structure in Λ . Let $B_{zr} = |\{j | j \in C_r \text{ and } \exists i \in C_z \text{ s.t. } (i, j) \in \mathcal{S}_\Lambda\}|$ be the number of columns in C_r with at least one active variable in (C_z, C_r) . Then $B = \sum_{z \neq r} |B_{zr}|$ is the number of times we need to recompute a column in Σ and Ψ while traversing off-diagonal blocks. This implies that coordinate descent for Λ costs $O((q+B)m_\Lambda K)$ for computing Σ , and $O((q+B)nq)$ for computing Ψ . As for alternating Newton coordinate descent, the cost of each individual coordinate update is $O(q)$. The overall cost is then $O((q+B)(m_\Lambda K + nq) + m_\Lambda q)$.

The dependence on B highlights how recognizing diagonal structure improves performance. In the best case where Λ becomes perfectly block-diagonal, $B = 0$ and the overall cost of updating Λ reduces to $O(qm_\Lambda K + nq^2 + m_\Lambda q)$. In the worst case where we need to recompute all q/k_Λ columns of Σ_{C_r} and Ψ_{C_r} in each of the off-diagonal blocks, $B \sim qk_\Lambda$ and the overall cost of updating all blocks is $O(k_\Lambda qm_\Lambda K + k_\Lambda nq^2 + m_\Lambda q)$.

A.3.2 Time Cost of Updating Θ

To sweep through all the blocks in Θ , we compute Σ only once while potentially computing columns of $\mathbf{S}_{\mathbf{xx}}$ multiple times. Thus, the cost of computing Σ is $O(qm_\Lambda K)$ and does not depend on sparsity in Θ . The cost of computing $\mathbf{V} = \Theta \Sigma$ is $O(qm_\Theta)$ and also does not depend on sparsity or the number of blocks. For the cost of computing $\mathbf{S}_{\mathbf{xx}}$, we assume that Θ has $\tilde{p} \leq p$ non-empty rows, so that the number of blocks with at least one active variable is at most $\tilde{p}k_\Theta$. Let $B = I_\phi(\mathcal{S}_{(i, C_r)})$ be the number of blocks (i, C_r) where we need to compute $\mathbf{S}_{\mathbf{xx}i}$. The cost of computing $\mathbf{S}_{\mathbf{xx}i}$ for each cache miss is $O(n\tilde{p})$. Thus, computing $\mathbf{S}_{\mathbf{xx}}$ for updating all blocks in Θ is $O(Bn\tilde{p})$ which is upper-bounded by $O(k_\Theta n\tilde{p}^2)$. The cost of each individual coordinate update is $O(\tilde{p} + q/k_\Theta)$. The overall cost is then $O(Bn\tilde{p} + qm_\Lambda K + qm_\Theta + m_\Theta(\tilde{p} + q/k_\Theta))$.

For large problems the time needed to compute $\mathbf{S}_{\mathbf{xx}}$ dominates. In the worst case where $\tilde{p} = p$ and graph clustering is ineffectual so that $B = k_\Theta p$, updating all blocks requires computing $\mathbf{S}_{\mathbf{xx}}$ a total of k_Θ times with cost $O(k_\Theta np^2)$. However, because we store only one row of $\mathbf{S}_{\mathbf{xx}}$ at a time, k_Θ will be small, even for problems with large p . In fact, for large sparse problems, the effect of sparsity can outweigh the additional k_Θ factor so that $Bn\tilde{p}$ can be smaller than np^2 .

A.4 Additional Results from Synthetic Data Experiments

We compare the performance of the different algorithms on synthetic datasets with different sample sizes n , using a chain graph structure with $p = 10,000$ and $q = 10,000$. Figure 5(a) shows that our methods run significantly faster than the previous method across all sample sizes. In Figure 5(b) we measure the accuracy in recovering the true chain graph structure in terms of F_1 -score for different sample sizes n . At convergence, F_1 -score was the same for all methods to three significant digits. As expected, the accuracy improves as the sample size increases.